In-Orbit Vicarious Calibration for Ocean Color and Aerosol Products

Menghua Wang
NOAA National Environmental Satellite, Data, and Information Service
Office of Research and Applications
E/RA3, Room 102, 5200 Auth Road, Camp Springs, MD 20746, USA

***Abstract*—It is well known that, to accurately retrieve the spectrum of the water-leaving radiance and derive the ocean color products from satellite sensors, a vicarious calibration procedure, which performs sensor in-orbit calibration for a whole system (the sensor and algorithms) is necessary. Both Sea-viewing Wide Field-of-view Sensor (SeaWiFS) and Moderate Resolution Imaging Spectroradiometer (MODIS) have employed in-orbit vicarious calibration procedure that uses the *in situ* measurements with the Marine Optical Buoy (MOBY) in the waters off Hawaii. Such method can also be applied to vicarious inter-calibrate other sensors. In addition to the ocean color products, aerosol optical property data over ocean are routinely retrieved from both SeaWiFS and MODIS measurements. The aerosol retrieval algorithm uses radiances measured at two near-infrared (NIR) wavelengths, at which the ocean appears black due to strong absorption by water, to estimate the aerosol optical properties and extrapolate these into the visible. The spectral information from two-band measurements is used to retrieve the most appropriate aerosol models. With the derived aerosol models, the aerosol optical thickness can then be estimated using the measured signal at 865 nm. In this paper, I outline the procedure for the in-orbit sensor vicarious calibration for the ocean color and aerosol products. Simulations that demonstrate the effectiveness of the vicarious calibration method on the derived ocean color and aerosol products are presented and discussed. Results of sensitivity studies that show effects of the calibration error at 865 nm, appropriateness of aerosol models, and the solar-sensor viewing geometry on the accuracy of the retrieved ocean color and aerosol optical properties are presented.**

I. INTRODUCTION

In the ocean color remote sensing, <10% of the sensor-measured radiance in the visible at satellite altitude is from the ocean near-surface water, and scattering from the atmosphere and the sea surface comprises the rest [1, 2]. This places very stringent requirements on the sensor's radiometric calibration, particularly in the blue bands. Even for a perfect atmospheric correction (i.e., effects of atmosphere and surface are accurately removed), the relative error in the derived ocean color spectrum will be at least 10 times the relative error in the sensor calibration. Thus, for an uncertainty of 5% in the retrieved water-leaving radiance in the blue, the uncertainty in the radiometric calibration of the sensor must be within ~0.5%. It is impossible to achieve such an uncertainty purely through the pre-launch sensor radiometric calibration in the laboratory. Even if this were possible, the launch process would likely cause unknown changes in the sensor's radiometric response. The key calibration procedure for the ocean color mission is the in-orbit vicarious calibration [3, 4]. The basic strategy is to account for all of the components of the top of atmosphere (TOA) radiance reflected from the ocean-atmosphere system by direct measurement or by prediction based on *in situ* measurements, radiative transfer, and scattering theory. The computed TOA radiances are then compared with the results from sensor-measured radiances. Any difference between the measured and computed TOA radiance is attributed to error in the calibration of the sensor, and calibration gain coefficients can be therefore derived to force the measurements and computations into confluence (the computed TOA radiance is considered as correct value).

Gordon [4] provided a strategy of the in-orbit vicarious calibration for the ocean color sensors. In this scheme, it is assumed that the longest wavelength band in the near-infrared (NIR) is perfectly calibrated, and then all other bands (shorter than the longest wavelength) are in effect calibrated with respect to this band. This is the relative calibration. Wang and Gordon [5] show that as long as the calibration error at the longest NIR band (i.e., 865 nm) is within ~5% in magnitude, the in-orbit vicarious calibration can produce the TOA radiances that are sufficiently accurate to retrieve water-leaving radiances with very good accuracy. This is completely independent of the initial pre-launch calibration uncertainty for all the shorter wavelengths (i.e., shorter than 865 nm). The in-orbit vicarious calibration has been successfully used to both the Sea-viewing Wide Field-of-view Sensor (SeaWiFS) [6] and the Moderate Resolution Imaging Spectroradiometer (MODIS) using the Marine Optical Buoy (MOBY) [7] for the ocean color products. The in-orbit vicarious calibration scheme can be also used for the vicarious inter-calibration between sensors [8].

In deriving the ocean color products from ocean color sensors (e.g., SeaWiFS), the aerosol effects must be accurately estimated and removed. Therefore, the SeaWiFS can also produce the aerosol optical property data, in particular, the aerosol optical thickness and Ångström exponent, over global ocean [1, 9].

In this paper, I briefly describe the procedure for the in-orbit sensor vicarious calibration for the ocean color and

Report Documentation Page

Form Approved
OMB No. 0704-0188

1. REPORT DATE	2. REPORT TYPE	3. DATES COVERED
25 JUL 2005	**N/A**	**-**

4. TITLE AND SUBTITLE	5a. CONTRACT NUMBER
In-Orbit Vicarious Calibration for Ocean Color and Aerosol Products	5b. GRANT NUMBER
	5c. PROGRAM ELEMENT NUMBER
6. AUTHOR(S)	5d. PROJECT NUMBER
	5e. TASK NUMBER
	5f. WORK UNIT NUMBER
7. PERFORMING ORGANIZATION NAME(S) AND ADDRESS(ES) **NOAA National Environmental Satellite, Data, and Information Service Office of Research and Applications E/RA3, Room 102, 5200 Auth Road, Camp Springs, MD 20746, USA**	8. PERFORMING ORGANIZATION REPORT NUMBER
9. SPONSORING/MONITORING AGENCY NAME(S) AND ADDRESS(ES)	10. SPONSOR/MONITOR'S ACRONYM(S)
	11. SPONSOR/MONITOR'S REPORT NUMBER(S)

12. DISTRIBUTION/AVAILABILITY STATEMENT
Approved for public release, distribution unlimited

13. SUPPLEMENTARY NOTES
See also ADM001850, 2005 IEEE International Geoscience and Remote Sensing Symposium Proceedings (25th) (IGARSS 2005) Held in Seoul, Korea on 25-29 July 2005. , The original document contains color images.

14. ABSTRACT

15. SUBJECT TERMS

16. SECURITY CLASSIFICATION OF:			17. LIMITATION OF ABSTRACT	18. NUMBER OF PAGES	19a. NAME OF RESPONSIBLE PERSON
a. REPORT	b. ABSTRACT	c. THIS PAGE			
unclassified	**unclassified**	**unclassified**	**UU**	**4**	

Standard Form 298 (Rev. 8-98)
Prescribed by ANSI Std Z39-18

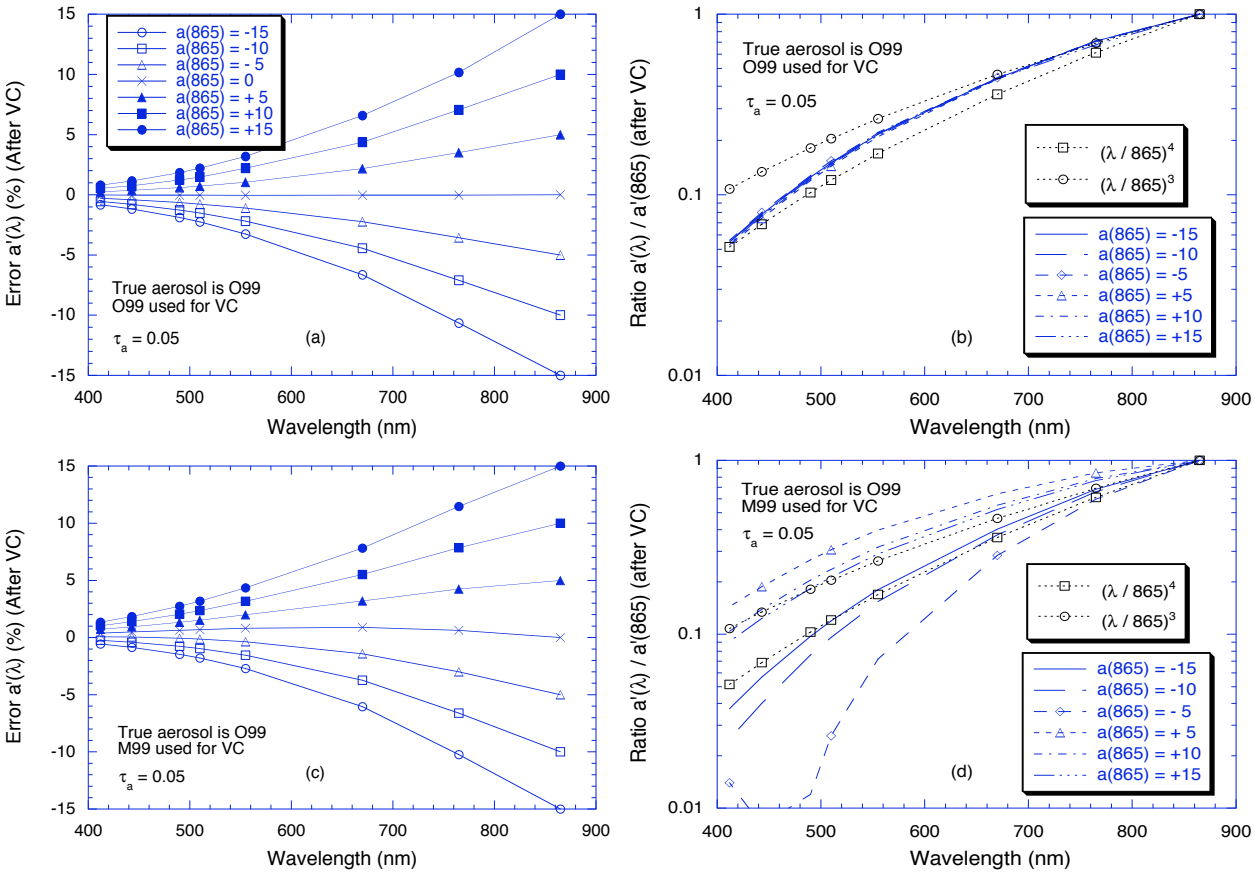

Figure 1. The residual calibration error $a'(\lambda)$ (%) (panels (a) and (c)) and ratio $a'(\lambda)/a'(865)$ (panels (b) and (d)) as a function of the wavelength for $a(865)$ values of ±5%, ±10%, and ±15%.

aerosol products. Discussions that explain physics of the relative vicarious calibration are provided. Examples from simulations that demonstrate the effectiveness of the vicarious calibration method on the derived ocean color and aerosol products are presented and discussed. In addition, results of sensitivity studies that show effects of the calibration error at 865 nm on the accuracy of the retrieved ocean color and aerosol optical properties are presented.

II. VICARIOUS CALIBRATION PROCEDURE

By using the reflectance $\rho = \pi L / F_0 \cos\theta_0$, where L is the radiance in the given viewing direction, F_0 is the extraterrestrial solar irradiance, and θ_0 is the solar zenith angle, the TOA reflectance for the ocean-atmosphere system, measured at a wavelength λ, can be written as [1]

$$\rho_t(\lambda) = \rho_r(\lambda) + \rho_A(\lambda) + t(\lambda)\rho_w(\lambda), \qquad (1)$$

where $\rho_r(\lambda)$, $\rho_A(\lambda)$, and $\rho_w(\lambda)$ are the reflectance contributions from the molecules (Rayleigh scattering), aerosols (including Rayleigh-aerosol interactions), and ocean waters (water-leaving reflectance), respectively. The *t(λ)* is the atmospheric diffuse transmittance that accounts for the effects of propagating water-leaving reflectance from the sea surface to the TOA [10]. It is computed with assumption that the backscattered radiance just beneath the sea surface is uniform, i.e., the water body is a Lambertian reflector observed just beneath the ocean surface. In the above equation, the surface sun glitter and whitecap terms have been ignored.

A set of realistic aerosol models is needed for computing $\rho_A(\lambda)$ in Eq. (1) (for the atmospheric correction). The current SeaWiFS and MODIS ocean color data processing uses 12 aerosol models for generating the aerosol lookup tables [9]. They are the Oceanic model with the relative humidity (RH) of 99% (denoted as O99), the Maritime model with RH of 50%, 70%, 90%, and 99% (denoted as M50, M70, M90, and M99), the Coastal model with RH of 50%, 70%, 90%, and 99% (denoted as C50, C70, C90, and C99), and the Tropospheric model with RH of 50%, 90%, and 99% (denoted as T50, T90, and T99). These models are from *Shettle and Fenn* [11], and represented well for the maritime ocean environment [12].

In the vicarious calibration (VC), the quantities of each term on the right hand side of Eq. (1) are estimated and summed, and the sensor calibration is adjusted to yield a value of $\rho_t(\lambda)$ that is in agreement with the estimation. Specifically, the Rayleigh reflectance $\rho_r(\lambda)$ is computed using atmospheric pressure and surface wind speed. The water-leaving reflectance $\rho_w(\lambda)$ is measured directly at the

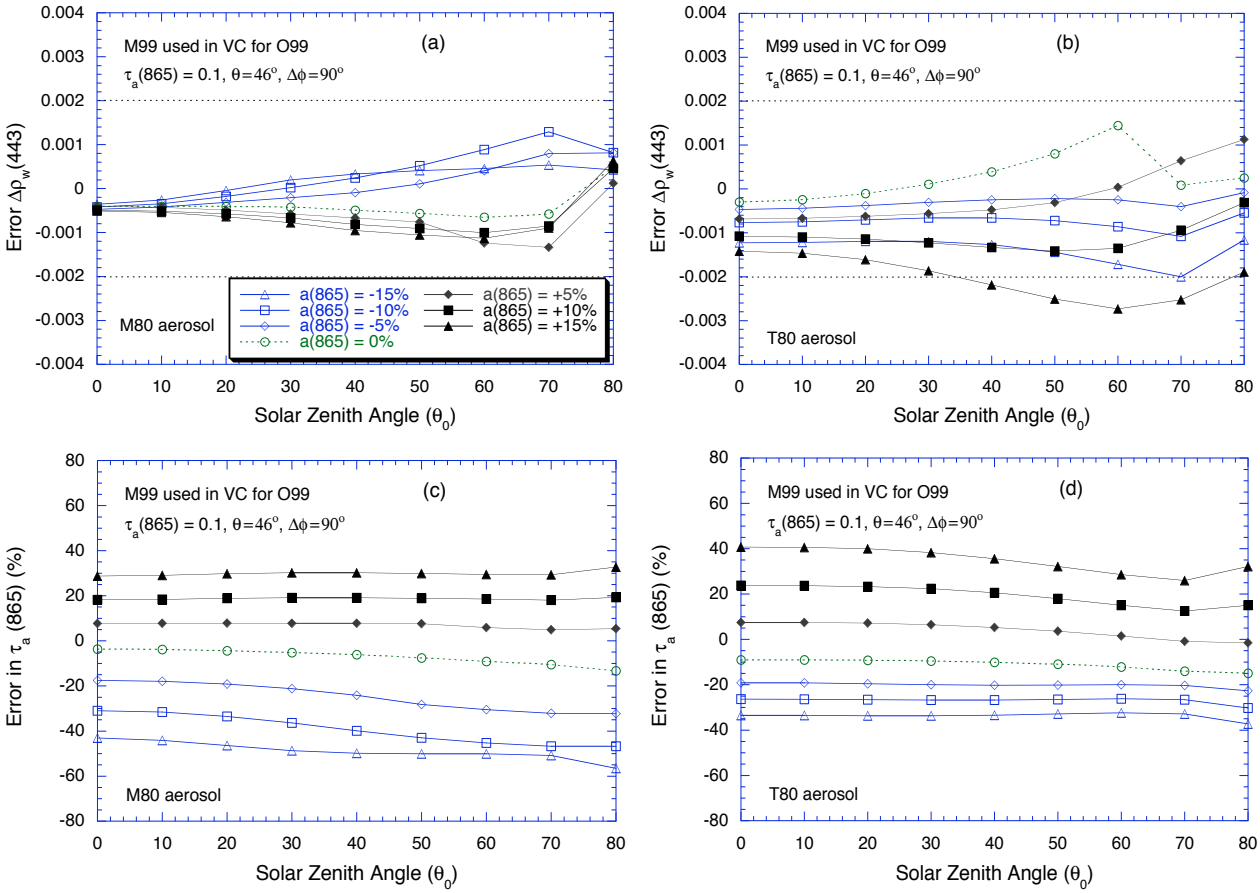

Figure 2. Errors in the derived water-leaving reflectance and aerosol optical thickness using the Gordon-Wang algorithm with the TOA reflectances modified by the VC procedure for various calibration uncertainties at 865 nm. (a) and (b) are errors in the derived water-leaving reflectance for M80 and T80 models, and (c) and (d) are errors (%) in the derived aerosol optical thickness at 865 nm.

VC site (e.g., MOBY) [7]. $\rho_A(\lambda)$ and $t(\lambda)$ are estimated using the radiative transfer theory with an aerosol model. The VC procedure can be schematically outlined as:

$$\rho_t^{(\mathrm{VC})}(\lambda) = \underbrace{\rho_r(\lambda)}_{\text{Computed}} + \underbrace{\rho_A(\lambda)}_{\text{VC aerosol model}} + t\underbrace{\rho_w(\lambda)}_{\text{in situ}}. \qquad (2)$$

The above is specifically for a VC site. We can write the sensor-measured TOA reflectance as:

$$\rho_t^{(M)}(\lambda) = \left[1+a(\lambda)\right]\rho_t^{(T)}(\lambda), \qquad (3)$$

where $\rho_t^{(M)}(\lambda)$ is the reflectance that would be measured by a sensor and $\rho_t^{(T)}(\lambda)$ is the TOA "true" reflectance. $a(\lambda)$ is the sensor calibration errors (before VC). After the VC, the sensor-measured TOA reflectance is modified as:

$$\rho_t^{(C)}(\lambda) = \left[1+a'(\lambda)\right]\rho_t^{(T)}(\lambda), \qquad (4)$$

where $\rho_t^{(C)}(\lambda)$ is the "Corrected" sensor-measured TOA reflectance and $a'(\lambda)$ is the residual calibration error after VC. Wang and Gordon [5] show that the residual calibration error $a'(\lambda)$ depends only on the solar-sensor geometry in VC site, the VC aerosol model, the VC in situ water-leaving reflectance measurements, and $a(865)$ value. The $a'(\lambda)$ does not depend on $a(\lambda)$ for $\lambda < 865$ nm. Note that $a'(865) = a(865)$ as it is assumed that 865 nm band is error free in the VC procedure [4, 5].

Figure 1 shows results of $a'(\lambda)$ and $a'(\lambda)/a'(865)$ as a function of wavelength for $a(865)$ values of ±5%, ±10%, and ±15%. Figs. 1(a) and 1(b) are results of $a'(\lambda)$ and $a'(\lambda)/a'(865)$ from a VC using a correct aerosol model (model O99), while Figs. 1(c) and 1(d) are results from an incorrect VC aerosol model (true O99, but M99 for VC). In Fig. 1, the VC has been carried out specifically for aerosol optical thickness of 0.05 with "true" aerosol model of O99, and solar-sensor geometry of 20°, 20°, and 90° for the solar-zenith, sensor-zenith, and relative azimuth angle, respectively. Figs. 1(b) and 1(c) also plot the curves of $(\lambda/865)^4$ and $(\lambda/865)^3$ that demonstrate basic physics of the VC procedure—the ratio of residual calibration error $a'(\lambda)/a'(865)$ varies according to more or less the inverse of the Rayleigh scattering, i.e., $(\lambda/865)^4$. The $a'(\lambda)$ in the visible is about an order less than $a'(\lambda)$ at 865 nm. Thus, using the outlined in-orbit VC scheme, for calibration uncertainty of ~5% at the 865 nm, the calibration uncertainty in the blue can be reduced to within ~0.5%.

III. EFFECTS ON THE DERIVED OCEAN COLOR AND AEROSOL PRODUCTS

To assess the efficacy of the VC scheme, simulations have been carried to evaluate the accuracy of the derived water-leaving reflectance $\rho_w(\lambda)$ and aerosol optical thickness $\tau_a(\lambda)$ using the TOA reflectances that have been modified with the VC gains, i.e., $\rho_t^{(C)}(\lambda)$ in Eq. (4), for the various VC cases (e.g., VC aerosol models, solar-sensor geometry, etc.), and various retrieval cases (e.g., aerosol optical properties, solar-sensor geometries, etc.). For the VC procedure, it was assumed that an incorrect aerosol model M99 was used for a "true" O99 model (realistic case). This is the same case as in Figs. 1(c) and 1(d). With the derived $a'(\lambda)$ for given $a(865)$ values (through the VC procedure), the TOA reflectance $\rho_t^{(C)}(\lambda)$ can be computed according to Eq. (4). In generating the testing data $\rho_t^{(C)}(\lambda)$, the Maritime and Tropospheric models with RH of 80% (M80 and T80) [11] were used. These two models are different from the 12 aerosol models used in generating aerosol lookup tables for the atmospheric correction and aerosol retrievals. With the generated $\rho_t^{(C)}(\lambda)$ values, the Gordon and Wang [1] atmospheric correction and aerosol retrieval algorithm was performed to derive the water-leaving reflectance $\rho_w(\lambda)$ and aerosol optical thickness at 865 nm $\tau_a(865)$.

Figure 2 provides examples of the retrieval results. Figs. 2(a) and 2(b) are uncertainties in the derived water-leaving reflectance at 443 nm for the M80 and T80 models, while Figs. 2(c) and 2(d) are errors (%) in the retrieved aerosol optical thickness for M80 and T80 models. These are for case of aerosol optical thickness $\tau_a(865)$ of 0.1 and for a specific sensor-viewing geometry (sensor-zenith angle of 46° and relative azimuth angle of 90°) with solar angles varying from 0°-80°. They are corresponding to the VC cases for $a(865)$ values of 0%, ±5%, ±10%, and ±15%, respectively.

Results in Figs. 2(a) and 2(b) show that the water-leaving reflectance at 443 nm can be retrieved accurately as long as the sensor calibration uncertainty at 865 nm $a(865)$ is within ~5%. In fact, for the M80 model, errors in the derived water-leaving reflectance are all within 0.002 and mostly within ±0.001 for $a(865)$ up to ±15%. For the T80 model, except some cases with larger solar zenith angles for $a(865) = +15\%$, the derived water-leaving reflectances are all accurate within ±0.002.

On the other hand, Figs. 2(c) and 2(d) show that error in the derived aerosol optical thickness at 865 nm is almost twice the magnitude as the calibration uncertainty $a(865)$, e.g., 5% in $a(865)$ leading to ~10% error in the derived aerosol optical thickness $\tau_a(865)$. This is because the aerosol scattering contributes ~50% of the sensor-measured TOA reflectance (Rayleigh scattering contributes another 50%). Calibration error in the TOA reflectance at 865 nm is equivalent to double the effect on the aerosol component. Therefore, to retrieve the aerosol optical thickness within error of 10%, $a(865)$ has to be within 5%.

ACKNOWLEDGMENT

This research was supported by NASA NPP and MODIS grants NNG04GE05A and NNG04HZ22C, and NOAA Internal Government Studies (IGS) C2NF1NP.

REFERENCES

[1] H. R. Gordon and M. Wang, "Retrieval of water-leaving radiance and aerosol optical thickness over the oceans with SeaWiFS: A preliminary algorithm," *Appl. Opt.*, vol. 33, pp. 443-452, 1994.

[2] H. R. Gordon, "Atmospheric correction of ocean color imagery in the Earth Observing System era," *J. Geophys. Res.*, vol. 102, pp. 17,081-17,106, 1997.

[3] R. H. Evans and H. R. Gordon, "CZCS system calibration: A retrospective examination," *J. Geophys. Res.*, vol. 99, pp. 7293-7307, 1994.

[4] H. R. Gordon, "In-orbit calibration strategy for ocean color sensors," *Rem. Sens. Environ.*, vol. 63, pp. 265-278, 1998.

[5] M. Wang and H. R. Gordon, "Calibration of ocean color scanners: How much error is acceptable in the near-infrared," *Remote Sens. Environ.*, vol. 82, pp. 497-504, 2002.

[6] J. R. E. Eplee, W. D. Robinson, S. W. Bailey, D. K. Clark, P. J. Werdell, M. Wang, R. A. Barnes, and C. R. McClain, "Calibration of SeaWiFS. II: Vicarious techniques," *Appl. Opt.*, vol. 40, pp. 6701-6718, 2001.

[7] D. K. Clark, H. R. Gordon, K. J. Voss, Y. Ge, W. Broenkow, and C. Trees, "Validation of atmospheric correction over the ocean," *J. Geophys. Res.*, vol. 102, pp. 17,209-17,217, 1997.

[8] M. Wang and B. A. Franz, "Comparing the ocean color measurements between MOS and SeaWiFS: A vicarious intercalibration approach for MOS," *IEEE Trans. Geosci. Remote Sens.*, vol. 38, pp. 184-197, 2000.

[9] M. Wang, K. D. Knobelspiesse, and C. R. McClain, "Study of the Sea-Viewing Wide Field-of-View Sensor (SeaWiFS) aerosol optical property data over ocean in combination with the ocean color products," *J. Geophys. Res.*, vol. 110, pp. D10S06, doi:10.1029/2004JD004950, 2005.

[10] H. Yang and H. R. Gordon, "Remote sensing of ocean color: assessment of water-leaving radiance bidirectional effects on atmospheric diffuse transmittance," *Appl. Opt.*, vol. 36, pp. 7887-7897, 1997.

[11] E. P. Shettle and R. W. Fenn, "Models for the Aerosols of the Lower Atmosphere and the Effects of Humidity Variations on Their Optical Properties," U.S. Air Force Geophysics Laboratory, Hanscom Air Force Base, Mass. AFGL-TR-79-0214, 1979.

[12] K. D. Knobelspiesse, C. Pietras, G. S. Fargion, M. Wang, R. Frouin, M. A. Miller, A. Subramaniam, and W. M. Balch, "Maritime aerosol optical properties measured by handheld sun photometers," *Remote Sens. Environ.*, vol. 93, pp. 87-106, 2004.